Author/s:
Cochrane, NJ;Iijima, Y;Shen, P;Yuan, Y;Walker, GD;Reynolds, C;Macrae, CM;Wilson, NC;Adams, GG;Reynolds, EC

Title:
Comparative study of the measurement of enamel demineralization and remineralization using transverse microradiography and electron probe microanalysis

Date:
2014-01-01

Citation:
Cochrane, N. J., Iijima, Y., Shen, P., Yuan, Y., Walker, G. D., Reynolds, C., Macrae, C. M., Wilson, N. C., Adams, G. G. & Reynolds, E. C. (2014). Comparative study of the measurement of enamel demineralization and remineralization using transverse microradiography and electron probe microanalysis. Microscopy and Microanalysis, 20 (3), pp.937-945. https://doi.org/10.1017/S1431927614000622.

MICROSCOPY AND MICROANALYSIS

Microscopy Society of America

CAMBRIDGE UNIVERSITY PRESS

Comparative study of the measurement of enamel demineralization and remineralization using transverse microradiography and electron probe microanalysis

Journal:	*Microscopy and Microanalysis*
Manuscript ID:	MAM-13-139.R2
Manuscript Type:	Original Article
Date Submitted by the Author:	n/a
Complete List of Authors:	Cochrane, Nathan; The University of Melbourne, Oral Health CRC, Melbourne Dental School, Bio21 Institute Iijima, Youichi; Nagasaki University, Graduate School of Biomedical Sciences, Unit of Social Medicine, Department of Oral Health Shen, Peiyan; The University of Melbourne, Oral Health CRC, Melbourne Dental School, Bio21 Institute Yuan, Yi; The University of Melbourne, Oral Health CRC, Melbourne Dental School, Bio21 Institute Walker, Glenn; The University of Melbourne, Oral Health CRC, Melbourne Dental School, Bio21 Institute Reynolds, Coralie; The University of Melbourne, Oral Health CRC, Melbourne Dental School, Bio21 Institute MacRae, Colin; CSIRO Minerals, Microbeam Laboratory Wilson, Nicholas; CSIRO Process Science and Engineering, Microbeam Laboratory Adams, Geoffrey; The University of Melbourne, Oral Health CRC, Melbourne Dental School, Bio21 Institute Reynolds, Eric; The University of Melbourne, Oral Health CRC, Melbourne Dental School, Bio21 Institute
Keywords:	Transverse microradiography, electron probe microanalyzer analysis, EPMA, TMR, remineralization, demineralization

Microscopy and Microanalysis revised MS MAM-13-139 (updated 11 December 2013)

Comparative study of the measurement of enamel demineralization and remineralization using transverse microradiography and electron probe microanalysis

Nathan J. Cochrane[a], Youichi Iijima[b], Peiyan Shen[a], Yi Yuan[a], Glenn D. Walker[a], Coralie Reynolds[a], Colin M. MacRae[c], Nicholas C. Wilson[c], Geoffrey G. Adams[a], Eric C. Reynolds[a*]

[a] Oral Health CRC, Melbourne Dental School, Bio21 Institute, The University of Melbourne, 720 Swanston Street, Victoria, 3010, Australia

[b] Nagasaki University Graduate School of Biomedical Sciences, Unit of Social Medicine, Department of Oral Health, 1-7-1 sakamoto, Nagasaki, 852-8588, Japan

[c] Microbeam Laboratory, CSIRO Process Science and Engineering, Bayview Avenue, Clayton, Victoria, 3168, Australia

Key words: Transverse microradiography (TMR), electron probe microanalyzer analysis (EPMA), remineralization, demineralization

Brief title: Enamel mineral measurements with TMR and EPMA

[*]**Corresponding author:** Professor EC Reynolds, Melbourne Dental School, The University of Melbourne, 720 Swanston Street, Victoria 3010, Australia. Tel: 61 3 9341 1547; Fax: 61 3 9341 1596; Email: e.reynolds@unimelb.edu.au

ABSTRACT

Transverse microradiography (TMR) and electron probe microanalysis (EPMA) are commonly used for characterizing dental tissues. TMR utilizes an approximately monochromatic X-ray beam to determine the mass attenuation of the sample which is converted to volume percent mineral (vol%min). An EPMA stimulates the emission of characteristic X-rays from a variable volume of sample (dependent on density) to provide compositional information. The aim of this study was to compare the assessment of sound, demineralized and remineralized enamel using both techniques. Human enamel samples were demineralized and part was subsequently remineralized. The same line profile through each demineralized lesion was analyzed using TMR and EPMA to determine vol%min and wt% elemental composition and atomic concentration ratio information respectively. The vol%min and wt% values determined by each technique were significantly correlated but the absolute values were not similar. This was attributable to the complex ultrastructural composition, the variable density of the samples analyzed and the non-linear interaction of the EPMA generated X-rays. EPMA remains an important technique for obtaining atomic ratio information but its limitations in determining absolute mineral content indicate that it should not be used in place of TMR for determining the mineral density of dental hard tissues.

INTRODUCTION

Dental caries is the prevalent disease process whereby net mineral is lost from the hard tissues of the teeth (Selwitz et al., 2007). New approaches to promote the net uptake of mineral back into these damaged areas are currently receiving much research interest (Cochrane et al., 2010). A variety of different methods can be used to measure this loss or gain of dental mineral including transverse microradiography (TMR), polarised light microscopy, microhardness determination and electron probe microanalysis (EPMA) with energy dispersive or wavelength dispersive spectrometry (ten Bosch & Angmar-Mansson, 1991). TMR is the standard method for the measurement of changes in mineral content of the dental hard tissues (ten Bosch & Angmar-Mansson, 1991). It usilizes a monochromatic X-ray beam to determine mass attenuation which is then converted to volume percent mineral (vol%min). EPMA can be used for the chemical analysis of samples with a high spatial resolution yielding both qualitative identification of elements and quantitative compositional information of micro-volumes (Landis, 1979). EPMA analysis is based on the emission of characteristic X-ray radiation of elements within a small volume of sample excited by the impact of a focused beam of electrons (Chu et al., 1989; Heinrich & Newbury, 1991) whose energies and relative abundance depend upon the composition of the sample.

EPMA has been used for the analysis of dental tissues ever since the technique was first introduced (Boyde et al., 1961). At this time it was appreciated that biological samples of variable density were difficult to analyse quantitatively (i.e. determine their elemental composition) such that it was described as a semi-quantitative technique (Boyde et al., 1961). However, more recently investigators have been using EPMA for quantifying the mineral content of dental hard tissues of variable density by measuring the weight percent (wt%)

composition of the major elements in the tissue and implying that their change indicates that demineralization or remineralization has occurred (Ab-Ghani et al., 2007; Baroni & Marchionni, 2011; Ngo et al., 2006; Yip et al., 1995). This approach has been studied by Ngo et al. (1997) who found that there was a strong correlation in the mineral distribution of the same defined lesions determined by EPMA and TMR and that there was no significant difference in the measurement of lesion depth as measured by the two techniques. However, the findings from the study by Ngo et al. (1997) are not consistent with ten Bosch and Angmar-Mansson (1991) who concluded that "microprobing methods are not appropriate for determining the absolute concentrations of the major constituents" in incipient caries lesions. This opinion was based on the fact that as the density varies across the lesion an EPMA can only be used to accurately quantify relative atomic concentration ratios. Given the frequency of use of EPMA in dental tissue analysis and the conflict in recommendations of EPMA as a quantitative technique the aim of this study was to conduct a detailed investigation into the relationship between the measurement of enamel demineralization and remineralization using EPMA compared with the standard method TMR.

MATERIALS AND METHODS

Preparation of enamel subsurface Lesions

Four extracted human teeth were obtained from oral surgeons and general practitioners with ethics approval (Dental Research Ethics Committee of Nagasaki University (authorized number: 0735)). The teeth were stored in a 10% v/v neutral phosphate buffered formalin solution for 2 weeks. Sound relatively planar buccal and lingual surfaces with minimal cracking, staining and fluorosis (as viewed under a dissecting microscope) were selected for analysis. Enamel

subsurface lesions were prepared by creating windows with nail varnish and then exposing those windows to a demineralization organic acid buffer (pH 4.5) containing 3.0 mM calcium and 1.8 mM phosphate for 3 days (Tanaka & Iijima, 2001). The enamel slabs were then treated with either 9000 ppm neutral fluoride, 9000 ppm acidic fluoride or 900 ppm neutral fluoride to encourage different patterns of remineralization. After this treatment the enamel slabs were immersed in a remineralization solution (pH 7.0) containing 3.0 mM calcium, 1.8 mM phosphate and no fluoride for 3 days at 37 ^{o}C (Tanaka & Iijima, 2001). One third of each window was left uncovered by nail varnish and then subjected to an acid resistance test in the same demineralization solution used to create the lesions for 3 days (Fig 1A). This process produced 12 lesions - 4 standardized demineralized lesions, 4 variable remineralized lesions and 4 variable acid challenged lesions to test the agreement of mineral quantification using TMR and EPMA.

Sample preparation for transverse microradiography

When treatment was completed, sections 200-300 μm thick were cut from the embedded enamel slab using an internal annulus saw microtome (Leitz 1600, Ernst Leitz Wetzlar, Germany). Planoparallel sections were then lapped down to 90 ± 1 μm using a RotoPol21/RotoForce4 lapping instrument (Struers, Denmark) with 1200 grit lapping paper. Each section, which contained the demineralized control lesion, remineralized lesion and the acid challenged lesion (Fig. 1A) was radiographed along with an aluminum stepwedge of 7 × 37.5 μm thick increments using Microchrome High Resolution glass plates (HTA Enterprises, Michrochrome Technology Products, San Jose, CA, USA) and nickel filtered copper Kα radiation at 20 kV, 20 mA for 12 min using a custom-manufactured TMR system (Diffraction Technologies, Mt Eliza, Vic, Australia). The X-ray source was a glass 1200W PANalytical fine-focus tube with a Cu target

(PANalytical, Condell Park, NSW, Australia). The X-ray tube was powered by a Spellman XLF -60 N 1200 generator (Spellman HV, Hauppauge, NY, USA) cooled with recirculated and refrigerated water using a Polyscience water chiller model 6706P (Polyscience, Niles, IL, USA). The Cu Kβ radiation was attenuated using a Ni filter. Each photographic glass plate was developed in Microchrome Developer D5 (1:4 dilution, Microchrome Technology Products, San Jose, CA, USA) for five min, placed into glacial acetic acid stop bath for 30 s and fixed in Microchrome Developer F4 (1:4 dilution, Microchrome Technology Products, San Jose, CA, USA) for five min.

Sample preparation for EPMA

The section of tooth X-rayed for TMR was embedded in epoxy resin (Epofix; Struers, Denmark) on a one inch specimen holder. The resin was flat polished to expose the enamel sections using 2400 grit abrasive paper. To achieve optical smoothness 3 µm and 1 µm diamond polishing pastes were used on a cloth pad with final finishing accomplished with a 0.25 µm aluminum oxide paste. All samples and standards were coated with 20 nm of carbon by carbon arc deposition using a Dynavac 300 coater.

Operating parameters for EPMA

The electron probe (8900R SuperProbe JEOL, Japan) was operated at a 15 kV accelerating voltage, 10 nA beam current, 40º take off angle. The elements measured were Ca, P, O, K, Na, Mg and F. Oxygen was measured by integrating across the peak and background was measured separately. Dwell times used for major (Ca, P, O) and minor elements (K, Na, Mg, F) were 10 or 20 s for the peak and 10 or 20 s for the background respectively per point. A synthetic

fluorapatite standard (manufactured by Charles M. Taylor) was used to calibrate the machine. The standards were analyzed using a 10 µm (defocused) and 2 µm (focused) diameter beam to calibrate the X-ray count intensity. The standards were halite (**Na**Cl), synthetic and natural (Wilberforce) fluorapatite ($\mathbf{Ca}_5(\mathbf{PO_4})_3\mathbf{F}$), Adularia ($\mathbf{K}AlSi_3O_8$) and Spinel ($\mathbf{Mg}Al_2O_4$). The synthetic fluorapatite had been chemically analyzed and had a calcium to phosphorous atomic ratio of 1.667 and a fluoride content of 3.70 wt%. Using the operating parameters defined above the synthetic fluorapatite and Wilberforce fluorapatite had a calcium to phosphorus ratio of 1.68 ± 0.02 and 1.69 ± 0.03 respectively. Given the greater variability of the natural fluorapatite standard the synthetic sample was used as the primary standard.

Quantitative line scans were collected across the lesions starting from sound enamel and traversing into the epoxy resin perpendicular to the surface layer. The two sigma detection limits for each of the elements were Ca 160 parts per million (ppm), P 1440 ppm, O 1000 ppm, K 70 ppm, Na 200 ppm, Mg 120 ppm and F 400 ppm. These equate to a two sigma percentage error of 0.3, 2.0, 0.5, 37, 6.4, 17 and 16 % respectively. Data were matrix corrected using a $\phi(\rho Z)$-Parabolic method correction procedure (Pouchou & Pichoir, 1984; Pouchou & Pichoir, 1991) implemented in STRATAGEM 3.0 thickness and compositional thin film analysis package, (SAMx, Saint Andre de la Roche, France, 1997). Fluorescence by the characteristic lines and by the continuum were corrected using this method for each line.

A variety of beam diameters were tested to determine the optimal beam current density for the analysis of enamel (Fig 1B). The beam diameter employed during collection of standards was a 10 µm spot whereas the diameter for analysis of lesions was 5 µm with a 5 µm step between points. Weight % of all elements was added to determine a total wt% of mineral in the tested region.

Monte Carlo modeling

Monte Carlo modeling was performed using CASINO 2.45 to estimate the interaction volume of the 15 kV electron beam interacting with apatite at four different densities (Drouin et al., 2007; Drouin et al., 1997; Hovington et al., 1997). The apatite densities that were used for the modeling were synthetic apatite [3.15 g/cm^3 (ten Bosch & Angmar-Mansson, 1991)], sound tooth enamel [2.63 – 2.77 g/cm^3 (Cochrane et al., 2012)] and demineralized enamel [1.26 – 2.38 g/cm^3 (Cochrane et al., 2012)].

Transverse microradiography image analysis

The radiographic images of the lesions that were taken prior to EPMA analysis were viewed via transmitted light using a Leica DM 5500B microscope (Leica, Germany). The images were acquired by a Progres® MF scan digital camera (Jentopik, Jena, Germany) under the control of Image-Pro Plus version 7.0 imaging software on a Sci-Tech Imaging Workstation (SciTech, Preston, VIC, Australia). The TMR image of each lesion was matched side by side to an optical image at the same magnification of the lesion surface after analysis by EPMA to locate the position of the line scan and allow the same area to be analyzed by TMR. The TMR analysis was performed across the lesions starting from the epoxy resin perpendicular to the surface layer and traversing into sound enamel. The demineralized, remineralized and acid challenged lesions and their neighboring areas of sound enamel were scanned using the program's line luminance function that gave readings in gray values. Each scan comprised 200 readings taken from the tooth surface to sound enamel. The start and end of the lesion were defined as the points where the mineral density was 20 and 95 % respectively that of the sound enamel (ten Cate et al., 1996).

The stepwedge image on each slide was scanned and the averaged step gray value readings were plotted against aluminum thickness. The readings of the tooth section images lay within the linear portion of the stepwedge curve and linear regression was used to convert the gray value data into values of equivalent thicknesses of aluminum. The section thicknesses were measured using a Nikon Digimicron MFC-101A micrometer (Nikon, Tokyo, Japan) to ± 1 μm and the volume % mineral data computed using the equation of Angmar *et al.* (1963) and the linear absorption coefficients of aluminum, organic matter plus water and apatite mineral (131.5, 11.3, and 260.5 respectively) as previously described (Walker et al., 2010). TMR data were averaged over 5 μm intervals to allow a direct comparison with the EPMA data that was acquired with this spatial resolution.

Data transformations

Total wt% mineral EPMA data were converted to vol%min assuming that the sound enamel wt% was equivalent to 86.2 vol%min (Angmar et al., 1963). The calcium wt% was determined from the TMR data at the various points across the lesion by assuming that sound enamel (86.2 vol%min) was composed of 37 wt% Ca (Angmar et al., 1963). The surface layer, lesion body and points of maximum and minimum mineral density are defined in Fig 2. It is noted that the transformation of TMR data to calcium wt% assumes that in the acid challenged, demineralized and remineralized regions both the removal of material and remineralization occur as stoichiometric apatite which has been shown previously (Cochrane et al., 2008).

Statistical analysis

Correlations between the profiles (EPMA total mineral wt% vs TMR vol%min), mineral content maxima and minima were determined by Pearson or Spearman's correlations. Differences between maxima and minima mineral content of the lesion as measured by TMR and EPMA were determined using paired t-tests with significance set at $\alpha = 0.05$. These analyses were conducted using SPSS version 17 (Statistical Package for the Social Sciences, SPSS Inc.) A Bland-Altman plot of vol%min as determined by TMR and EPMA was performed in Stata (version 1.1, StataCorp, College Station, TX, USA).

RESULTS

The effect of various beam size diameters on the appearance of the enamel samples can be seen in Fig 1B. The 2 µm beam diameter appeared to produce ablation marks to the sample. The 5 µm beam diameter with 5 µm step distance was chosen for analysis of the samples as minimal beam effects were observed and this diameter and step size allowed numerous points to be analyzed across the depth of the lesion.

Plots of the mineral content determined by TMR (vol%min) and EPMA (total mineral wt% and total mineral wt% expressed as vol%min) are shown in Fig 2 for a representative demineralized (A), remineralized (B) and acid challenged lesion (C). It can be seen that all profiles for a given lesion follow a similar pattern with maxima in the surface layer, minima in the lesion body and then returning to sound levels. Although the profiles were all correlated significantly (correlation coefficients > 0.76, $p<0.001$) the absolute values were not similar with significant differences existing between the maxima ($p<0.001$) and minima ($p<0.001$) mineral content values as determined by TMR and EPMA. This can be seen in Fig 3A where the differences between the measurements are plotted for all lesions against depth. Large differences

were found predominantly in the lesion body and the surface layer. The Bland-Altman plot (Fig 3B) shows that there is a tendency for the mineral content of sound enamel to be underestimated whereas the lesion body measurements are overestimated by EPMA. The mean difference between the measurements at the lesion maxima and minima were 10.2 ± 6.4 vol%min and 21.0 ± 15.1 vol%min respectively with EPMA consistently providing the higher values as seen in Fig 2. An example of the major wt% elemental composition determined by EPMA of a typical demineralized lesion is shown in Fig 4. For comparison the wt% Ca determined from the TMR data is shown to again highlight the discrepancies in the quantitative measurements produced by the two techniques. The lesion depth of demineralized enamel as determined by TMR and EPMA was 84 ± 4 μm and 71 ± 11 μm respectively.

Exposure to the remineralization solution returned mineral to the body of the lesion and the second acid challenge produced more net mineral loss (Fig 2). The calcium to phosphorus atomic wt% ratio determined using EPMA across the lesions and into sound enamel was similar for the demineralized (2.01 ± 0.05), remineralized (2.02 ± 0.05) and acid challenged lesions (2.02 ± 0.05).

Monte Carlo modeling of the 15 kV electron beam is shown in Fig 5. This shows that as density changes from that of pure apatite to lower density apatite similar to that found in demineralized enamel, the interaction volume of the beam increases.

DISCUSSION

Sample preparation for EPMA is very important as a smooth surface for analysis is essential. The instrument operating parameters are also essential as electron bombardment deposits energy into the sample that can cause effects as seen in Fig 1B, and can repel or attract minor elements to the

beam (Edie & Glick, 1980). In this study the beam produced by a 15 kV and 10 nA source focused into a 2 µm beam diameter appeared to produce sample ablation. For this reason a larger diameter beam was chosen to distribute the energy across a greater volume and reduce the potential damage. Additionally, detection of minor elements were monitored for 2 min with the 5 µm beam diameter to ensure that the sample was stable in the beam and that elements were not attracted or repelled from the site of analysis. A 5 µm step size was also chosen to ensure high spatial resolution but also to move far enough away from the preceding area analyzed to avoid any beam damaged sample.

It is important to appreciate that EPMA and TMR are measuring different things. In the case of an EPMA the electron beam will penetrate into the sample a constant mass distance which is proportional to the energy of the electrons. As the enamel subsurface lesions tested in this study had variable mineral content the beam will have penetrated to different depths as the density changed. Monte Carlo modeling of this using the density of synthetic apatite (3.15 g/cm^3 (ten Bosch & Angmar-Mansson, 1991)), sound enamel (2.63 - 2.77 g/cm^3 (Cochrane et al., 2012)), and demineralized enamel (1.26 - 2.38 g/cm^3 (Cochrane et al., 2012)) clearly shows how the interaction volume changes (Fig 5). With the beam settings used in this study the interaction volume was limited to the outermost 5 µm of the sample but varied by up to approximately 100% between sound (2 µm) and demineralized enamel (4 µm). Furthermore, if polishing incorporates debris into pores or damages the outermost surface then this may influence the generated results given the shallow interaction volume. EPMA is measuring the elemental composition of a variable volume of the outermost material dependent on its density. TMR on the other hand is the projection of approximately monochromatic X-rays through the full thickness (90 ± 1 µm) of the sample to yield the total mineral content per defined volume.

The EPMA total mineral wt% profiles correlated with the TMR vol%min profiles, Fig 2, with correlation coefficients of 0.76 to 0.94, all of which were significant. This agrees with the findings of Ngo et al. (1997) although these authors did not provide correlation coefficients. Assessing the mineral profiles and maxima and minima values in Fig 2 shows that there was less contrast within the EPMA profile compared with the TMR profile, which is the standard method for quantifying enamel mineral content (ten Bosch & Angmar-Mansson, 1991). The Bland-Altman plot shows that there were smaller differences between the TMR and the EPMA measurements when the enamel was more mineralized (> 85 vol%min) and that this difference increased as the mineral content decreased (Fig 3B). Enamel is composed of apatite crystallites arranged into prisms and during demineralization the organic acid of the demineralization buffer diffuses down interprismetric spaces to dissolve crystallites to produce voids or porosities described as a subsurface demineralized lesion (Figs 1A and 2A). Although the majority of the dissolved apatite ions will diffuse out into the demineralization buffer bulk solution the porosities of the lesion will still contain the organic acid (e.g. lactic acid) or anion of the acid (e.g. lactate) that produced the subsurface lesion as well as some of the dissolved apatite ions. Upon sample drying these ions would precipitate as salts (e.g. calcium lactate) in the lesion spaces. It is assumed that these precipitated salts do not contribute significantly to the composition of the sample such that EPMA analysis should not show any detectable variation in wt% of either Ca or P in the lesion body. However, this is clearly not the case as the EPMA shows a detectable drop in wt% of both Ca and P in the body of the lesion (Fig 4). It has been shown previously that demineralization affects the enamel ultrastructure by increasing interprismatic spaces and changing individual crystallites by their dissolution from their peripheries or down their c-axis centre (Yanagisawa & Miake, 2003). Furthermore, remineralization of demineralized crystallites

is not uniform with ion deposition into central defects and onto the crystal periphery further increasing the irregularity of the crystallites (Cochrane et al., 2010; Yanagisawa & Miake, 2003). This creates areas of variable porosity with non-uniform sizes and spatial distribution. This may result in charge accumulation in the sample and non-linear interactions of the generated X-rays as shown by Sorbier et al. (1999) who studied porous media. Cazaux (2004) has shown that trapped charge of a few 10^{-3} C/m^2 is sufficient to induce an electrical field of 10^5 V/cm which may lead to internal slowing down of the primary electrons and a reduction in the generation of characteristic and continuous X-ray quanta. To determine if the drop in total weight percent was due to subsurface charging, X-ray spectra of both sound enamel and demineralized lesions were collected and compared (Fig 6). The combined spectra showed no discernible difference between the bremsstrahlung indicating that subsurface charging was not the cause of the problem. This suggests that the difference in the total weight percent sample composition is due mainly to the reduction in density associated with the increased porosity of the lesions. This reduction in density between sound and demineralized enamel can be up to a factor of four with the significantly increased porosities of the demineralized enamel containing calcium organic acid anion salts described above. The sound enamel will more closely approximate the apatite standards which likely explains the closer agreement of results for quantification of mineral in the sound enamel. However, across the depth of the lesion density decreased and porosity increased hence the sample became less similar to the standards used, contributing to the lack of concordance of absolute mineral content values between TMR and EPMA as suggested by ten Bosch and Angmar-Mansson (1991). The density/porosity effect will lead to a reduction in the correlation between TMR (vol%min) and the total wt% EPMA profiles as the EPMA encounters differing compositions compared with sound enamel. Hence, care must be taken in the

interpretation of the quantitative wt% information determined using EPMA of demineralized tooth enamel.

Comparing relative atomic ratios from EPMA data can minimize the density effect by assuming that each major element is likely to have been reduced by the same proportion as the density reduces. The atomic wt% ratio of calcium to phosphorus determined in this study closely matches that obtained by Frank et al. (1966) who found a ratio of 2.02 ± 0.02 for unerupted enamel and that of Wei (1970) who found a similar value for subsurface enamel. Given that the samples used in this study were polished to remove the outer surface enamel prior to lesion formation or treatment, the starting substrate would have been comparable to unerupted enamel. The ratio of calcium to phosphorus across the lesion was found to be stable for demineralized, remineralized and acid challenged enamel once again in agreement with the findings of Ngo et al. (1997) and those of Wei (1970). This is consistent with apatite being the depleted mineral phase during demineralization with a resultant loss of calcium and phosphate ions in this ratio and then the subsequent return of apatite in the same ratio during remineralisation. As ratio assessments are unaffected by local density differences this is a strength of the EPMA technique (ten Bosch & Angmar-Mansson, 1991).

CONCLUSIONS

EPMA can provide important relative compositional ratio information of samples as used by a number of authors for different purposes. However, use of this technique to quantify mineral content changes or quantify wt% elemental composition across enamel samples of variable density is highly problematic. The drawbacks include: the variable interaction volume, the non-uniform porosity causing density variations and an observed reduction of the generated X-rays

and the low interaction volume for inhomogeneous samples. It may be that charging can be minimized (with conductive embedding materials) or corrected to improve quantification but to the authors knowledge this approach has not been used in the study of dental tissues. The measurement of lesion depth may be conducted with EPMA if a sufficiently small spot size is used to have high spatial resolution although the reduced contrast may make determination of the base of the lesion more difficult. EPMA remains an important technique for obtaining both elemental concentrations and ratios but its limitations in determining absolute mineral content shown here indicate that it should not be used in place of TMR for the determination of mineral density of dental hard tissues.

REFERENCES

AB-GHANI, Z., NGO, H. & MCINTYRE, J. (2007). Effect of remineralization/demineralization cycles on mineral profiles of Fuji IX Fast *in vitro* using electron probe microanalysis. *Aust. Dent. J.* **52**, 276-281.

ANGMAR, B., CARLSTROM, D. & GLAS, J.E. (1963). Studies on the ultrastructure of dental enamel. IV. The mineralization of normal human enamel. *J Ultrastruct Res* **8**, 12-23.

BARONI, C. & MARCHIONNI, S. (2011). MIH supplementation strategies: prospective clinical and laboratory trial. *J Dent Res* **90**, 371-376.

BOYDE, A., SWITSUR, V.R. & FEARNHEAD, R.W. (1961). Application of the scanning electron-probe x-ray microanalyser to dental tissues. *J Ultrastruct Res* **5**, 201-207.

CAZAUX, J. (2004). About the mechanisms of charging in EPMA, SEM, and ESEM with their time evolution. *Microsc Microanal* **10**, 670-684.

CHU, J.S., FOX, J.L., HIGUCHI, W.I. & NASH, W.P. (1989). Electron probe micro-analysis for subsurface demineralization and remineralization of dental enamel. *J Dent Res* **68**, 26-31.

COCHRANE, N.J., ANDERSON, P., DAVIS, G.R., ADAMS, G.G., STACEY, M.A. & REYNOLDS, E.C. (2012). An X-ray microtomographic study of natural white-spot enamel lesions. *J Dent Res* **91**, 185-191.

COCHRANE, N.J., CAI, F., HUQ, N.L., BURROW, M.F. & REYNOLDS, E.C. (2010). New approaches to enhanced remineralization of tooth enamel. *J Dent Res* **89**, 1187-1197.

COCHRANE, N.J., SARANATHAN, S., CAI, F., CROSS, K.J. & REYNOLDS, E.C. (2008). Enamel subsurface lesion remineralisation with casein phosphopeptide stabilised solutions of calcium, phosphate and fluoride. *Caries Res.* **42**, 88-97.

DROUIN, D., COUTURE, A.R., JOLY, D., TASTET, X., AIMEZ, V. & GAUVIN, R. (2007). CASINO V2.42: a fast and easy-to-use modeling tool for scanning electron microscopy and microanalysis users. *Scanning* **29**, 92-101.

DROUIN, D., HOVINGTON, P. & GAUVIN, R. (1997). CASINO: A new Monte Carlo code in C language for electron beam interactions— Part II: Tabulated values of the mott cross section. *Scanning* **19**, 20-28.

EDIE, J.W. & GLICK, P.L. (1980). Electron irradiation effects in the EPMA quantitation of organic specimens. *Scan Electron Microsc*, 271-284.

FRANK, R.M., CAPITANT, M. & GONI, J. (1966). Electron probe studies of human enamel. *J Dent Res* **45**, 672-682.

HEINRICH, K.F.J. & NEWBURY, D.E. (1991). *Electron probe quantitation*. New York: Plenum Press.

HOVINGTON, P., DROUIN, D. & GAUVIN, R. (1997). CASINO: A new Monte Carlo Code in C language for electron beam interaction — Part I: Description of the program. *Scanning* **19**, 1-14.

LANDIS, W.J. (1979). Application of electron probe X-ray microanalysis to calcification studies of bone and cartilage. *Scan Electron Microsc*, 555-570.

NGO, H., RUBEN, J., ARENDS, J., WHITE, D., MOUNT, G.J., PETERS, M.C., FALLER, R.V. & PFARRER, A. (1997). Electron probe microanalysis and transverse microradiography studies of artificial lesions in enamel and dentin: a comparative study. *Adv Dent Res* **11**, 426-432.

NGO, H.C., MOUNT, G., MC INTYRE, J., TUISUVA, J. & VON DOUSSA, R.J. (2006). Chemical exchange between glass-ionomer restorations and residual carious dentine in permanent molars: an *in vitro* study. *J Dent* **34**, 608-613.

POUCHOU, J.L. & PICHOIR, F. (1984). A new model for quantitative x-ray microanalysis. Part I: Application to the analysis of homogeneous samples. *Rech Aerosp* **3**, 13-38.

POUCHOU, J.L. & PICHOIR, F. (1991). Quantitative analysis of homogeneous or stratified microvolumes applying the model (PAP). In *Electron Probe Quantification*, Heinrich, K. F. J. and Newbury, D. E. (Eds.), pp. 31-76. New York Plenum Press.

SELWITZ, R.H., ISMAIL, A.I. & PITTS, N.B. (2007). Dental caries. *Lancet* **369**, 51-59.

SORBIER, L., ROSENBERG, E., MERLET, C. & LLOVET, X. (1999). EPMA of Porous Media: A Monte Carlo Approach. *Microchimica Acta* **132**, 189-199.

TANAKA, K. & IIJIMA, Y. (2001). Acid resistance of human enamel in vitro after bicarbonate application during remineralization. *J Dent* **29**, 421-426.

TEN BOSCH, J.J. & ANGMAR-MANSSON, B. (1991). A review of quantitative methods for studies of mineral content of intra-oral caries lesions. *J Dent Res* **70**, 2-14.

TEN CATE, J.M., DUNDON, K.A., VERNON, P.G., DAMATO, F.A., HUNTINGTON, E., EXTERKATE, R.A., WEFEL, J.S., JORDAN, T., STEPHEN, K.W. & ROBERTS, A.J. (1996). Preparation and measurement of artificial enamel lesions, a four-laboratory ring test. *Caries Res.* **30**, 400-407.

WALKER, G.D., CAI, F., SHEN, P., ADAMS, G.G., REYNOLDS, C. & REYNOLDS, E.C. (2010). Casein phosphopeptide-amorphous calcium phosphate incorporated into sugar confections inhibits the progression of enamel subsurface lesions *in situ*. *Caries Res.* **44**, 33-40.

WEI, S.H. (1970). Electron microprobe analyses of the remineralization of enamel. *J Dent Res* **49**, 621-625.

YANAGISAWA, T. & MIAKE, Y. (2003). High-resolution electron microscopy of enamel-crystal demineralization and remineralization in carious lesions. *J. Electron Microsc.* **52**, 605-613.

YIP, H.K., BEELEY, J.A. & STEVENSON, A.G. (1995). Mineral content of the dentine remaining after chemomechanical caries removal. *Caries Res.* **29**, 111-117.

FIGURE LEGENDS

Figure 1. (A) A TMR image of an enamel sample with the three treated regions: the bottom third that has been demineralized; the middle third that was demineralized and then remineralized; and, the top third that underwent demineralization, remineralization and then had another exposure to the demineralization solution (acid challenge). The lesions shown are 80 μm deep. The white lines represent the middle of that lesion third that was analyzed with TMR and EPMA. (B) Secondary electron image of an enamel cross-section containing a demineralized lesion showing four line profiles using different beam diameters. Line 1 - 10 μm with a 10 μm step (far right); line 2 - 2 μm with a 5 μm step (second right); line 3 - 5 μm with a 5 μm step (second left); and line 4 - 5 μm with a 10 μm step (far left). In all cases beam effects can be seen. Ablation appeared to be occurring with the white circles in line 2 (shown by white arrow). Line 3 was chosen for analysis of samples as beam effects were judged to be acceptable and spatial resolution was relatively high.

Figure 2. Plots of the mineral content determined by TMR (vol%min) and EPMA (total mineral wt% and total mineral expressed as vol%min) for a representative demineralized (A), remineralized (B) and acid challenged lesion (C) from one tooth. In A: the surface layer (SL) is from 0 μm to the maxima (max) at ≈10 μm; the lesion body (LD) is from ≈10 μm to ≈75 μm with the minima (min) at ≈50 μm; the sound enamel is from ≈75 μm onwards; and the lesion depth (LD) is from 0 to ≈75 μm.

Figure 3. Difference between mineral content measurement expressed as vol%min determined by EPMA and TMR as a function of depth (A) and as a Bland-Altman plot (B). The diagonal

line in B is a line of best fit for the data points indicating that the measurements are not concordant and that a relationship exists between the mineral content and the difference between the two techniques. The large dashed line in B is the mean difference between the two measurements and the two small dashed lines are the Bland-Altman upper and lower limits of agreement.

Figure 4. The wt% profiles of the major elements determined by EPMA for a representative demineralized sample. Additionally, the wt% Ca profile determined by transforming the TMR data is shown to indicate the profile differences produced by the two techniques.

Figure 5. Monte Carlo modeling of the interaction of a 15 kV electron beam with four different densities of hydroxyapatite. At higher densities the interaction volume flattens and significantly reduces in depth. Monte Carlo modeling was performed using CASINO 2.45 (Drouin et al., 2007).

Figure 6. Energy dispersive x-ray spectra collected on both sound enamel and demineralized lesion were compared. The x-ray spectra were collected with an accelerating voltage of 15 kV, a beam current of 10 nA, the beam was defocused to 10 microns and each spectrum was collected for 30 seconds.

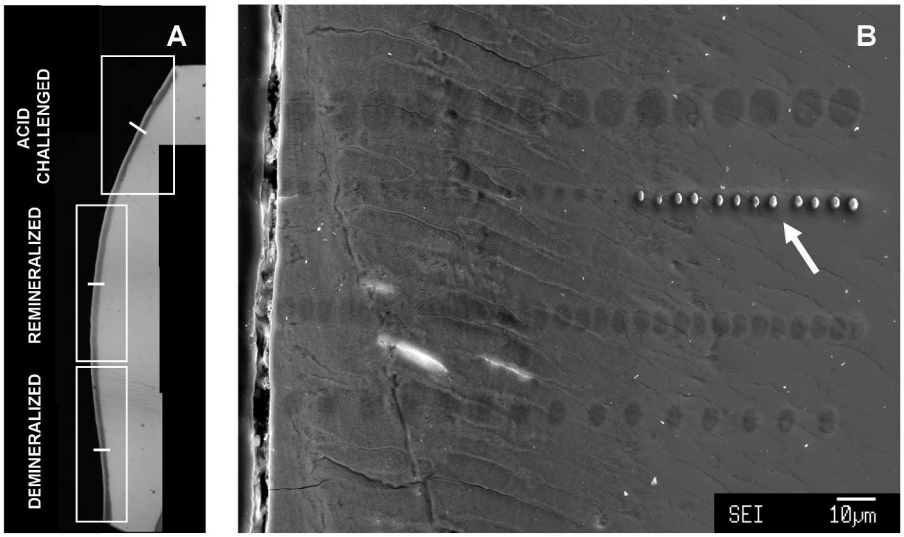

380x380mm (205 x 205 DPI)

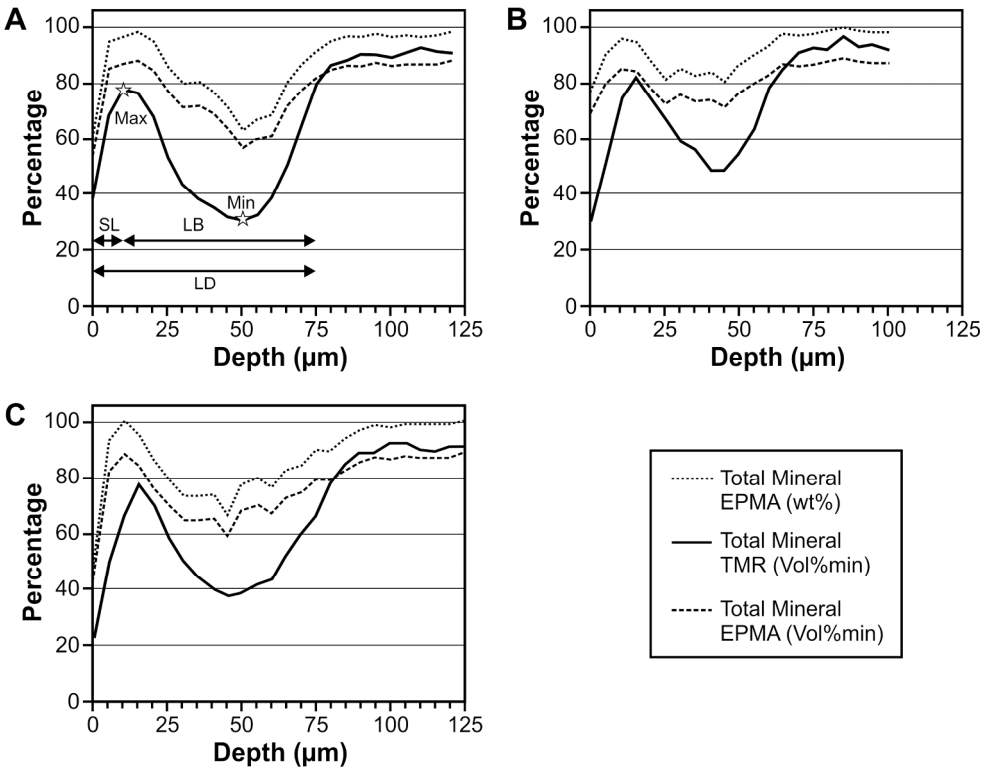

206x159mm (299 x 299 DPI)

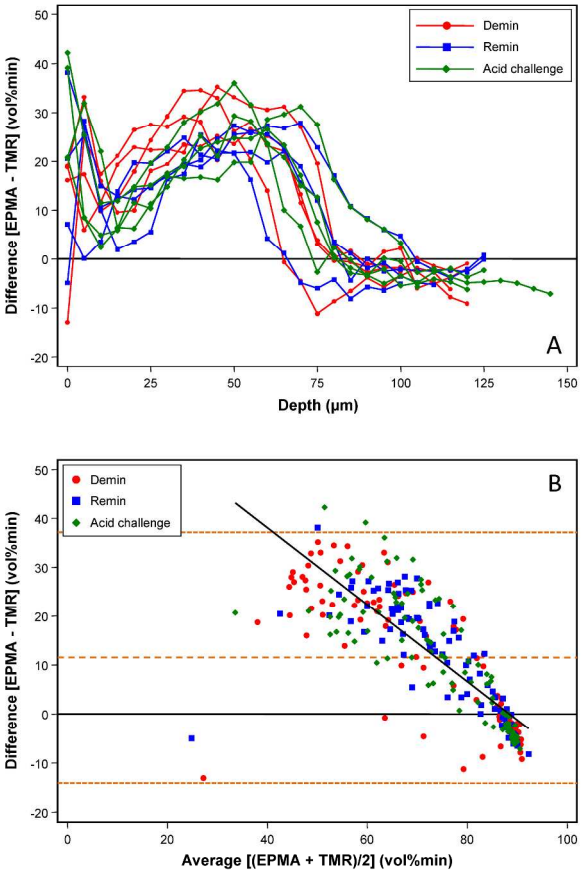

275x397mm (300 x 300 DPI)

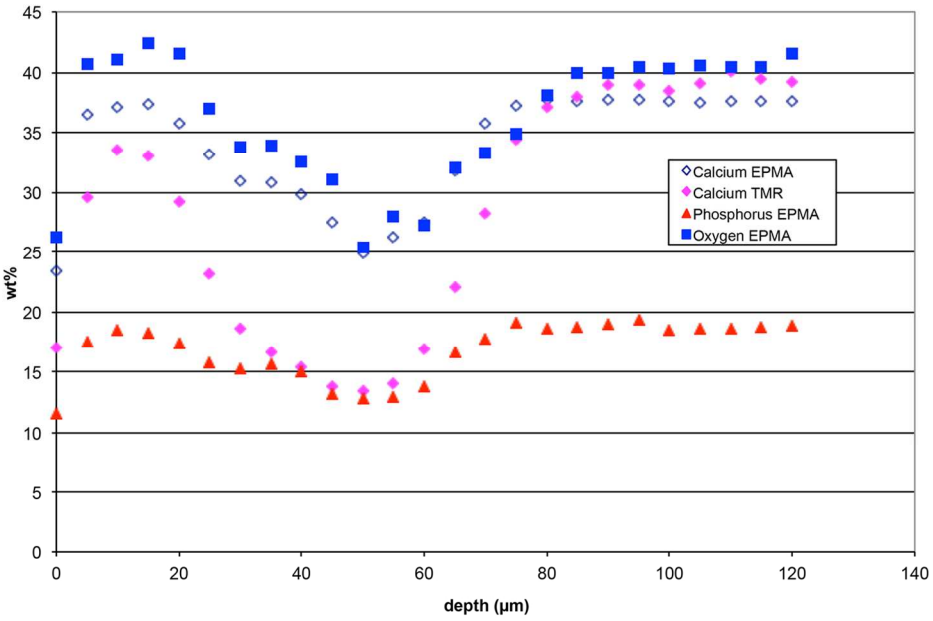

128x87mm (300 x 300 DPI)

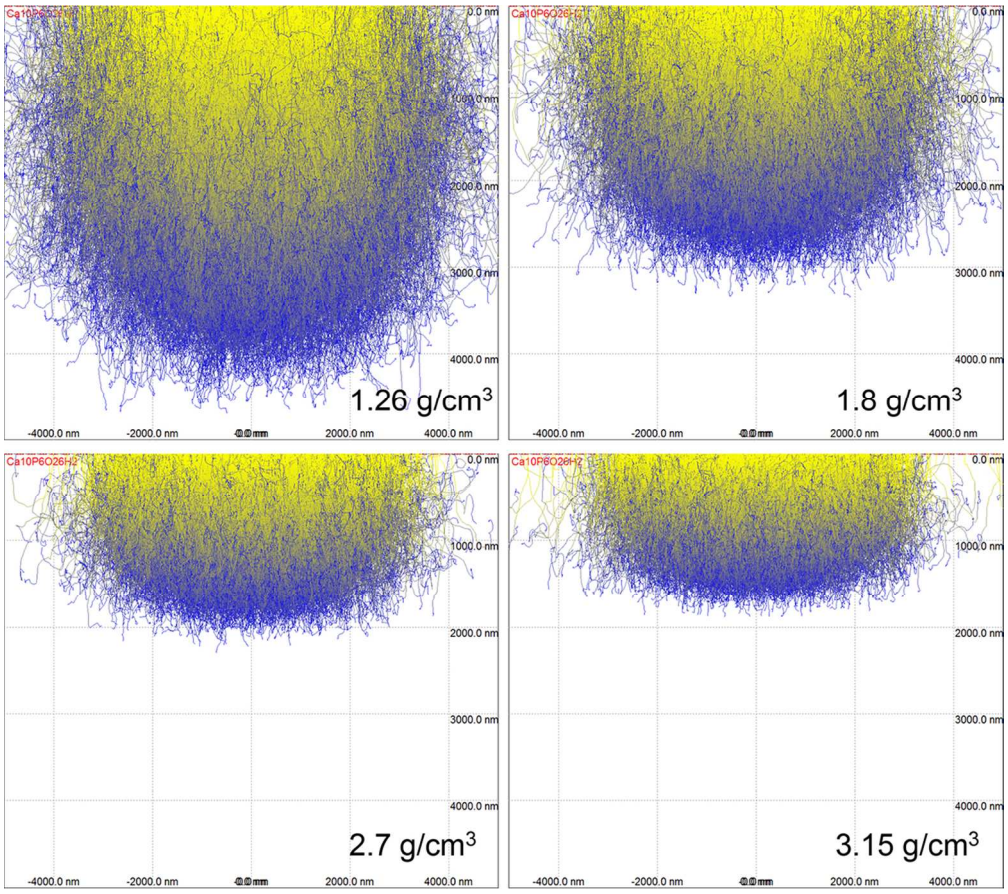

109x96mm (300 x 300 DPI)

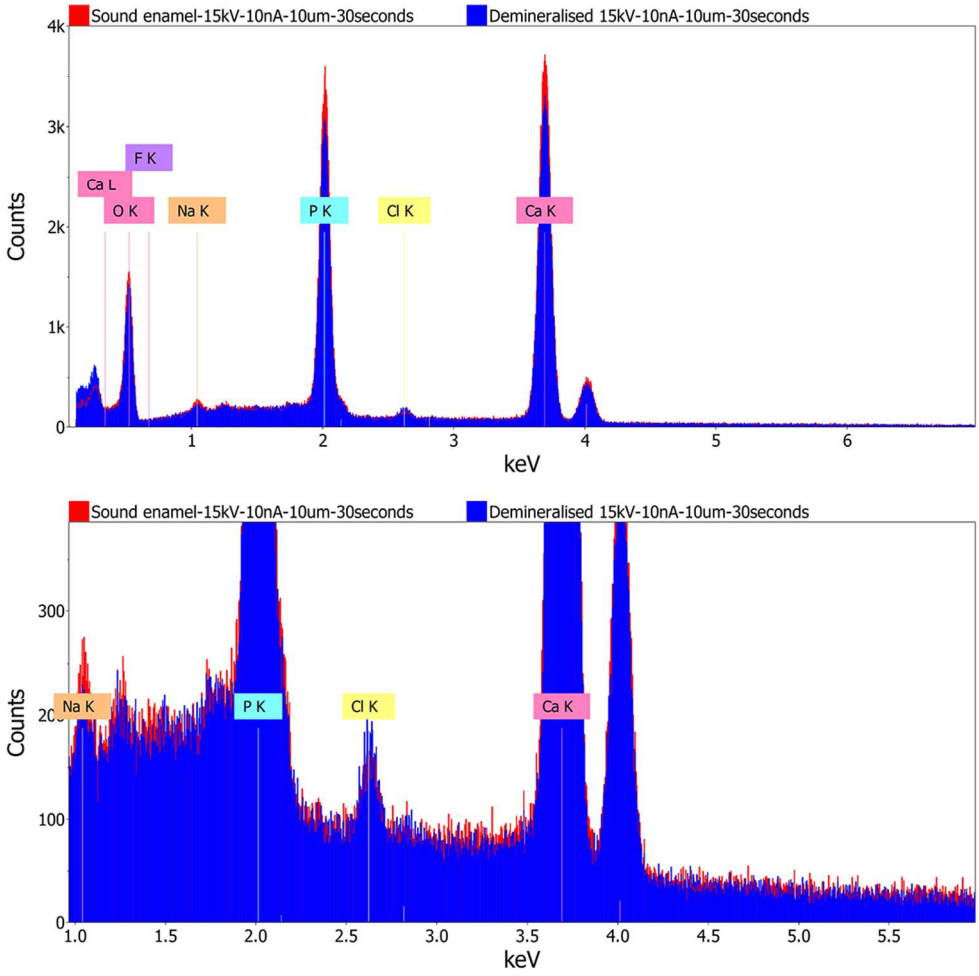

105x109mm (300 x 300 DPI)